

Postnatal epithelium and mesenchyme stem/progenitor cells in bioengineered amelogenesis and dentinogenesis



Nan Jiang^{a,b}, Jian Zhou^b, Mo Chen^b, Michael D. Schiff^b, Chang H. Lee^b, Kimi Kong^b, Mildred C. Embree^b, Yanheng Zhou^{a,**}, Jeremy J. Mao^{b,*}

^a Department of Orthodontics, Peking University School & Hospital of Stomatology, 22 Zhongguancun Nandajie, Haidian District, Beijing 100081, PR China

^b Columbia University Medical Center, Center for Craniofacial Regeneration (CCR), 630 W. 168 St. – PH7E, New York, NY 10032, USA

ARTICLE INFO

Article history:

Received 22 September 2013

Accepted 21 November 2013

Available online 15 December 2013

Keywords:

Epithelial

Mesenchymal

Stem cells

BMP

Wnt

Tooth regeneration

ABSTRACT

Rodent incisors provide a classic model for studying epithelial–mesenchymal interactions in development. However, postnatal stem/progenitor cells in rodent incisors have not been exploited for tooth regeneration. Here, we characterized postnatal rat incisor epithelium and mesenchyme stem/progenitor cells and found that they formed enamel- and dentin-like tissues *in vivo*. Epithelium and mesenchyme cells were harvested separately from the apical region of postnatal 4–5 day rat incisors. Epithelial and mesenchymal phenotypes were confirmed by immunocytochemistry, CFU assay and/or multi-lineage differentiation. CK14+, Sox2+ and Lgr5+ epithelium stem cells from the cervical loop enhanced amelogenin and ameloblastin expression upon BMP4 or FGF3 stimulation, signifying their differentiation towards ameloblast-like cells, whereas mesenchyme stem/progenitor cells upon BMP4, BMP7 and Wnt3a treatment robustly expressed Dspp, a hallmark of odontoblastic differentiation. We then control-released microencapsulated BMP4, BMP7 and Wnt3a in transplants of epithelium and mesenchyme stem/progenitor cells in the renal capsule of athymic mice *in vivo*. Enamel and dentin-like tissues were generated in two integrated layers with specific expression of amelogenin and ameloblastin in the newly formed, *de novo* enamel-like tissue, and DSP in dentin-like tissue. These findings suggest that postnatal epithelium and mesenchyme stem/progenitor cells can be primed towards bioengineered tooth regeneration.

© 2013 Elsevier Ltd. All rights reserved.

1. Introduction

Tooth develops upon interactions between epithelium and mesenchyme cells through distinctive morphological stages [1]. Rodent incisors continuously grow throughout postnatal life and have been robustly utilized as a classic model to study tooth development. Epithelium stem cells cluster in the cervical loop in the apical region of the rodent incisor, and differentiate into ameloblasts or enamel-forming cells [2]. This apical epithelium stem cell niche in the rodent incisor is regulated by cascades of signaling pathways including BMPs, Wnt, SHH and FGFs [3], and shares similarities to the hair follicle stem cell niche [4,5]. Continuous self-renewal and differentiation of epithelium and mesenchyme stem

cells in the rodent incisor replenish enamel and dentin, and sustain continuous growth and eruption of rodent incisors. However, this powerful model of self-renewing epithelium and mesenchyme stem cells in the rodent incisor has not been harnessed towards tooth regeneration.

Cell source is a central impediment for tooth regeneration in patients and has stimulated numerous investigations [6]. Mouse embryonic tooth germ cells, specifically E10 dental epithelium or E14.5 dental mesenchyme, can clearly initiate tooth morphogenesis [6]. Mouse E14.5 dental mesenchyme, when combined with oral epithelium of toothless chicks, gave rise to a developing tooth organ [7]. Reconstitution of E10 dental epithelium with postnatal bone marrow stromal cells also led to formation of a tooth organ [8]. E14.5 dental epithelium and mesenchyme cells, when reconstituted in a collagen gel, not only formed a tooth germ in organ culture, but also generated an erupted tooth when transplanted into the socket of an extracted adult tooth in the mouse [9,10]. Recently, E14.5 mouse dental mesenchyme, when reconstituted into cell sheets with iPS-like cells formed tooth-like structures [11,12]. Reconstituted mouse embryonic dental mesenchyme cells

* Corresponding author. Center for Craniofacial Regeneration (CCR), Columbia University, 630 W. 168 St. – PH7E – CDM, New York, NY 0032, USA. Tel.: +1 212 305 4475; fax: +1 212 342 0199.

** Corresponding author. Tel.: +86 10 82195381; fax: +86 10 62173402.
E-mail address: jmao@columbia.edu (J.J. Mao).

with human gingival epithelial cells formed developing tooth roots [13].

Despite the remarkable progress, the human equivalent to E10 to E14.5 mouse embryonic tooth germ cells, or ~3 month human embryonic tooth germ cells, are not applicable in human patients. A postnatal, somatic cell source with or without cellular programming is necessary for human applications of whole tooth regeneration, given severe safety concerns over and virtual impossibility in the application of embryonic tooth germ cells in patients [6]. Thus, a postnatal cell source that can yield amelogenesis and dentinogenesis is critically needed. Effort has been made to search for postnatal stem/progenitor cells that can be utilized in the regeneration of individual tooth structures including dentin, cementum and/or dental pulp or tooth roots [14–17]. However, little is understood about the potential for postnatal stem/progenitor cells in driving amelogenesis and odontogenesis. Thus, the objective of the present study was to investigate whether postnatal dental stem/progenitor cells can be manipulated for tooth regeneration. We hypothesized that postnatal dental stem/progenitor cells retain some of the capacity as pre-natal cells towards amelogenesis and odontogenesis.

2. Materials and methods

2.1. Isolation and culture of epithelium and mesenchyme stem/progenitor cells

Following IACUC approval, 4/5-day-old, post-natal Sprague–Dawley rats were sacrificed to isolate incisor epithelium and mesenchyme cells [18]. Briefly, the

mandible was aseptically removed (Fig. 1A) and digested in 2% collagenase (Gibco, Carlsbad, CA) in Dulbecco's Modified Eagle's Medium (DMEM: Invitrogen, Carlsbad, CA) at 4 °C overnight. The epithelium layer with the cervical loop was carefully separated from dental mesenchyme under dissection microscope (Fig. 1B, C). The cervical loop, which harbors dental epithelium stem cell niche [2], was illustrated in Fig. 1B (arrowhead). The isolated dental epithelium was further digested with 0.3-mg/mL collagenase and 0.4-mg/mL dispase (Gibco) for 30 min in Hank's Balanced Salt Solution and then filtered through a 40- μ m cell sieve. Single cell suspension was cultured in LHC-9, serum-free epithelium growth medium with 1% antibiotics/antimicrotics.

Dental mesenchyme was isolated under dissection microscope by a surgical cut in the apical region (dashed line in Fig. 1C) at a location directly posterior to the newly formed dentin. The isolated dental mesenchyme was minced and digested with 0.3-mg/mL collagenase and 0.4-mg/mL dispase for 30 min in DMEM, filtered through a 40- μ m cell sieve with single cells cultured in DMEM with 10% FBS and 1% antibiotics/antimicrotics.

2.2. Immunocytochemistry

Dental epithelium cells were cultured 5 days and fixed in 4% paraformaldehyde. Fixed cells were treated with 0.1% Triton X-100 (Sigma–Aldrich, St. Louis, MO) for 5 min, incubated with blocking buffer for 60 min (Oddssey, Lincoln, NE), and further incubated with primary antibodies at 4 °C overnight, including anti-cytokeratin 14 (CK14) mouse monoclonal IgG (1:100, Santa Cruz Biotechnology, Santa Cruz, CA), anti-Sox2 rabbit polyclonal IgG (1:200, Cell Signaling, Danvers, MA), anti-Lgr5 mouse monoclonal IgG (1:100, Origene, Rockville, MD), anti-Notch 1 rabbit polyclonal IgG (1:400, Millipore, Billerica, MA), anti-alkaline phosphatase rabbit polyclonal IgG (1:400, Abcam, Cambridge, MA, US), anti-ameloblastin rabbit polyclonal IgG (1:500, Santa Cruz Biotechnology) and anti-amelogenin mouse monoclonal IgG (1:500, Santa Cruz Biotechnology). Alexa Fluor[®] 555 Donkey Anti-Mouse IgG (H + L), Alexa Fluor[®] 488 Goat Anti-Mouse IgG (H + L) and FITC-conjugated goat anti-rabbit IgG (1:1000) were applied for 60 min. Cells were sealed with Vecta shield mounting

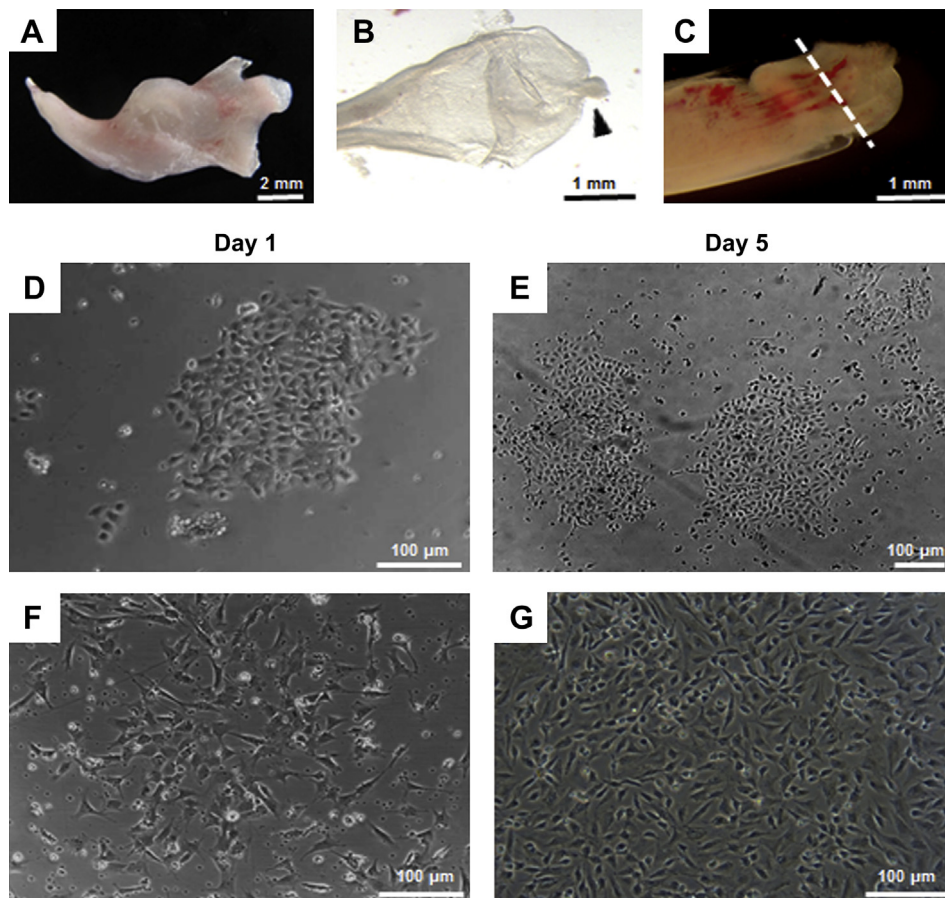


Fig. 1. Microdissection and subculture of rat dental epithelium and mesenchyme cells from 4 to 5 day postnatal rat incisors. A) Surgically removed mandible from a Sprague–Dawley rat showing erupted incisor. B) The dental epithelium layer with the cervical loop was carefully separated from dental mesenchyme under dissection microscope. The arrowhead shows distinctive structure of the cervical loop, which harbors dental epithelium stem cell niche. C) Dental mesenchyme was isolated with a surgical cut in the apical regions (dashed line) immediately posterior to the newly formed dentin. D, E) Dental epithelium stem cells grew into typical pebble-like colonies and propagated in LHC-9, serum-free medium in five days. F, G) Dental mesenchyme stem cells showed typical spindle shape, fibroblast-like morphology during passing.

medium containing DAPI diluted 1:2000. Mouse embryonic stem cells, embryonic kidney epithelial cells and rat incisor ameloblasts were used as positive controls. Blocking buffer was used to replace primary antibodies as a negative control.

2.3. Multi-lineage differentiation of dental mesenchyme cells

For odontogenic/osteogenic differentiation, passage 1 dental mesenchyme cells were cultured to confluence in DMEM with 10% FBS, 5 mM β -glycerophosphate, 50- μ M L-ascorbic acid 2-phosphate, 10-nM dexamethasone and 1% antibiotics/antimicrotics (Sigma), followed by fixation with 4% PFA in 2 wks. Cells were stained with 1% Alizarin red-S (Sigma) to detect mineral nodules. For adipogenesis, passage 1 dental mesenchyme cells were treated with adipogenic differentiation medium (Cyagen, Sunnyvale, CA) and cultured to confluence for 2 wks, followed by fixation with 4% PFA and stained with Oil red O. Total RNA was extracted from 3 independent samples for assaying odontogenesis/osteogenesis and adipogenesis markers by quantitative, real-time, reverse-transcription polymerase chain-reaction (qRT-PCR).

2.4. CFU-F assay

Mesenchyme cells were seeded on 35-mm cell culture dishes (Nalgene Nunc, Rochester, NY) to allow colony formation, with non-adherent cells removed after 4 h. Following 21 days, the flasks were stained with 0.1% crystal violet (Merck, Darmstadt, Germany) to illustrate CFU units.

2.5. BrdU labeling

Mesenchyme cells were cultured with 10- μ M BrdU (5-bromodeoxyuridin) (Invitrogen) for 4 h and then fixed with 4% PFA and treated with 0.1% Triton X-100. Alexa Fluor[®] 488 Goat Anti-Mouse IgG (H + L) was applied as a secondary antibody. Cells were sealed with Vecta shield mounting medium containing DAPI diluted 1:2000.

2.6. qRT-PCR

Total RNA was isolated using TRIzol (Invitrogen) per manufacturer's protocol. Briefly, 20% chloroform was added and centrifuged for 15 min. The aqueous, RNA-containing phase was separated and mixed with 0.5-ml isopropyl alcohol and 20- μ g glycogen. Following 10-min incubation, samples were centrifuged to form a pellet, washed with 75% ethanol, and resuspended in dH₂O. Complementary DNA (cDNA) was synthesized using the iScript cDNA synthesis kit (Bio-Rad, Hercules, CA). qRT-PCR was performed using TaqMan Assay Protocol (Applied Biosystems, Carlsbad, CA): hold for 2 min at 50 °C, hold for 10 min at 95 °C, and 50 cycles of melt for 15 s at 95 °C and anneal/extend for 1 min at 60 °C. All reactions were run in triplicates. Primers from Applied Biosystems were Rn01166223_m1 for amelogenin, Rn00563718_m1 for ameloblastin, Rn01413959_m1 for enamelin, Rn02132391_s1 for dspp, Rn01512298_m1 for Runx2, Rn00440945_m1 for PPAR γ , and Rn01775763_g1 for GAPDH. RNA expression was normalized to GAPDH and the control.

2.7. Microencapsulation of BMP4, BMP7 and Wnt3a and cells reconstitution

Microspheres of poly (D,L-lactic-co-glycolic acid) (PLGA, Sigma, St. Louis, MO) of 50:50 were prepared following our previous work [19,20]. 250 mg PLGA was dissolved into 1 mL chloroform, and 50 μ l of recombinant human BMP4 (R&D Systems, Minneapolis, MN), 50 μ l recombinant human BMP7 (R&D Systems) and 50 μ l recombinant human Wnt3a (R&D Systems) were mixed with 1 mL PLGA solution. Control microspheres contained only PBS with 0.1% bovine serum albumin. Then 2 mL of 1% polyvinyl alcohol (PVA) was added in PLGA solution, followed by 1 min mixing. A total of 100 mL of 2% isopropanol was added to the final emulsion and stirred for 2 h. Microspheres were stored in liquid nitrogen and lyophilized for at least 48 h before use. Before cell reconstitution, microspheres were deposited into a 30- μ l gel drop using Cellmatrix type I-A (Nitta, Osaka, Japan).

Dental epithelium and mesenchyme cells were reconstituted after 5–7 day culture [9]. Monolayer cells were washed in PBS and digested with 0.25% trypsin (Invitrogen) 5 min at 37 °C to isolate single cells. Epithelium and mesenchyme cells were injected into a gel drop at a density of 2×10^5 cells. Reconstituted gels were incubated with 380 μ l/well DMEM supplemented with 10% FBS (Invitrogen) and 50 μ g/mL ascorbic acid (Sigma) at 37 °C with 5% CO₂ for 2 days.

2.8. Surgical transplantation and tissue preparation

Following IACUC approval, we implanted cell encapsulated gel drops in the renal capsule in athymic nude mice (2-month-old, weighing 40–50 g; Harlan, Indianapolis, IN). Following 8-wk *in vivo* implantation, all samples were harvested and immersed in 4% paraformaldehyde for 24 h, followed by decalcification in 0.5 M EDTA (pH 7.4) for 7 days, embedded in paraffin and cut into 5- μ m sections. Randomly selected sections were used for hematoxylin and eosin as well as immunohistochemistry.

2.9. Immunofluorescence

Tissue samples were incubated with anti-ameloblastin rabbit polyclonal IgG (1:500, Santa Cruz Biotechnology), anti-amelogenin mouse monoclonal IgG (1:500, Santa Cruz Biotechnology) and anti-DSP polyclonal IgG (1:200, Santa Cruz

Biotechnology) overnight at 4 °C. Secondary antibodies FITC-conjugated goat anti-rabbit IgG (1:1000) and FITC-conjugated donkey anti-goat IgG (1:1000) were applied for 60 min.

2.10. Statistical analysis

All quantitative data were treated with one-way ANOVA with Bonferroni corrections upon confirmation of normal data distribution, with significance of $p \leq 0.05$.

3. Results

Microdissection separated the cervical loop in the epithelium envelope (arrowhead in Fig. 1B) from the underlying mesenchyme (Fig. 1C) in the postnatal 4–5 day incisor (Fig. 1A). Epithelium and mesenchyme cells of the tooth germ were separately isolated, and sub-cultured in different, chemically defined media as described above. Epithelium cells grew into typical pebble-like colonies (Fig. 1D, E), and propagated in LHC-9 medium, with little sign of mesenchyme cell contamination (Fig. 1E). In contrast, mesenchyme cells showed typical spindle shape, fibroblast-like morphology during passaging (Fig. 1F, G).

The isolated epithelium cells readily expressed epithelial phenotypes. Cells isolated from dental epithelium, following 5-day culture, overwhelmingly expressed CK14 (Fig. 2A–C), accounting for ~95% of all cultured epithelium cells (data not shown). Furthermore, dental epithelium cells expressed Sox2 (Fig. 2D–F) and Lgr5 (Fig. 2G–I), accounting for ~20% of all cultured epithelium cells (data not shown). The isolated dental epithelium cells also expressed alkaline phosphatase (Alp) (Fig. 2J–L) and Notch1 (Fig. 2D–I), accounting for ~12% and ~6% of all cultured epithelium cells, respectively. Few cells expressed ameloblastin (Fig. 2P–R) or amelogenin (Fig. 2S–U), indicating that the majority of the isolated epithelium cells are stem/progenitor cells, and have not differentiated into ameloblasts.

The isolated dental mesenchyme cells formed single cell colonies (Fig. 3A), indicating their ability to self-renew. Some of the isolated mesenchyme cells were BrdU positive (Fig. 3B) and continued to proliferate in culture, accounting for ~21% of total cells. Mesenchyme cells differentiated into osteoblast/odontoblast-like cells that formed mineral nodules (Fig. 3D) and robustly expressed Dspp, osteocalcin and Runx2 (Fig. 3E), with control in Fig. 3C. Moreover, dental mesenchyme cells differentiated into adipocyte-like cells, a lineage not native to dental mesenchyme, accumulated abundant lipid vesicles (Fig. 3G), and robustly expressed peroxisome proliferator-activated receptor γ (PPAR γ) (Fig. 3H), an adipogenesis transcriptional factor, with control in Fig. 3F.

We selected BMP4, BMP7, FGF3 and FGF10 proteins to augment amelogenesis of the isolated epithelium cells, given the pivotal roles of their corresponding genes in amelogenic differentiation [21,22]. Indeed, amelogenesis genes were upregulated including ameloblastin, amelogenin, and enamelin in 3 days (Fig. 4A–C). Strikingly, ameloblastin was upregulated ~65 fold upon BMP4 treatment (Fig. 4A). Also notable were increases in mRNA expression of amelogenin and enamelin upon BMP4 and FGF3 treatments (Fig. 4B, C), as well as ameloblastin upon FGF3 treatment (Fig. 4A). Collectively, BMP4 and FGF3 may augment amelogenesis *in vivo*.

In parallel, BMP4, BMP7 and Wnt3a were adopted to augment odontogenesis in the isolated postnatal dental mesenchyme cells, given the pivotal roles of their corresponding genes in promoting odontoblastic differentiation [3]. Indeed, odontogenesis genes were up-regulated including Dspp, alkaline phosphatase (Alp) and osteocalcin in 3 days (Fig. 4D–F). Remarkably, Dspp, a hallmark of odontoblastic differentiation, showed over 50-fold increases upon BMP4 (100 ng/mL) and BMP7 (50 and 100 ng/mL) treatments (Fig. 4D). Osteocalcin, a late stage odontogenesis/osteogenesis gene,

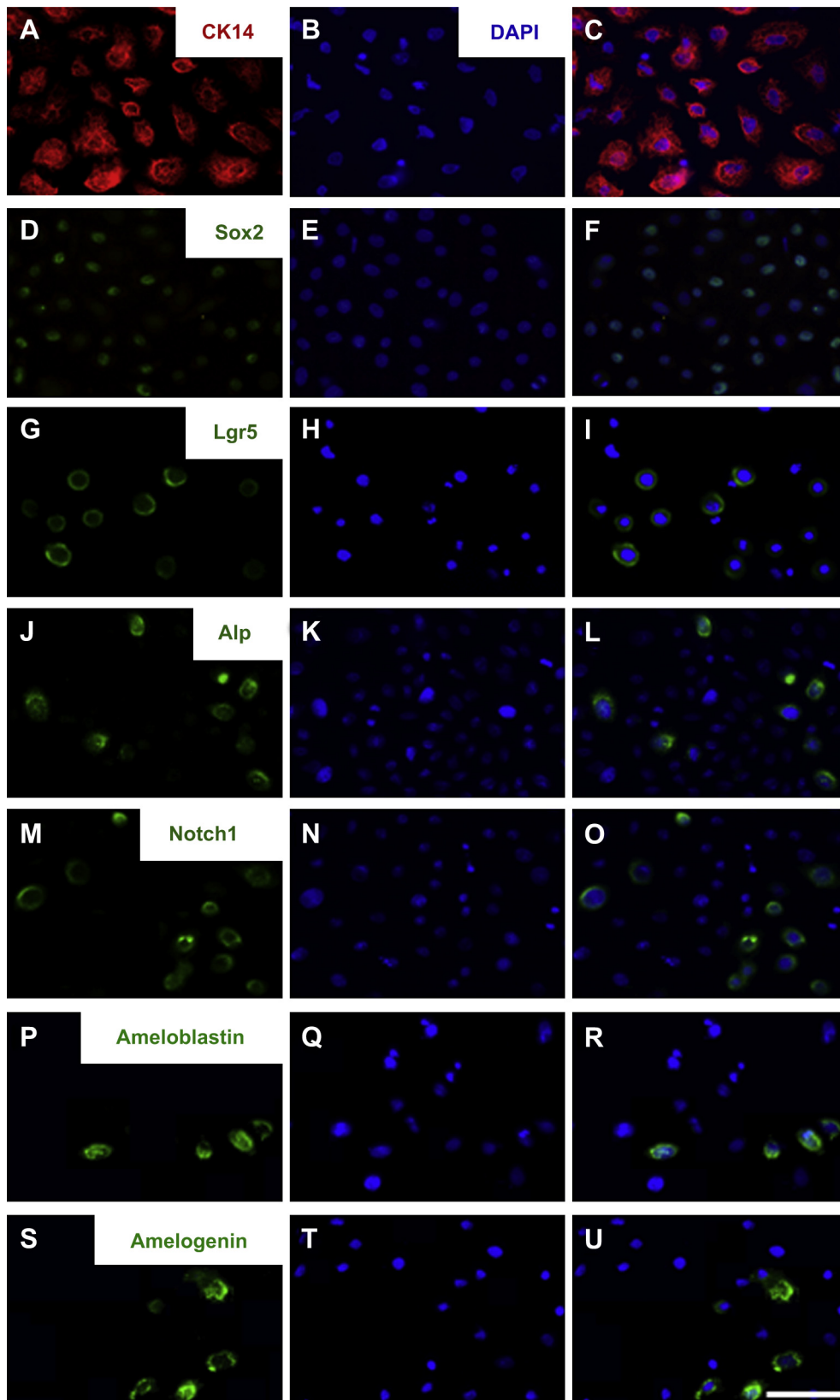


Fig. 2. Immunocytochemistry of epithelium stem cell phenotype. A–C) Isolated dental epithelium following 5-day culture, overwhelmingly expressed CK14; D–F) Sox2; G–I) Lgr5; J–L) alkaline phosphatase (Alp); M–O) Notch1; P–R) ameloblastin; S–U) amelogenin.

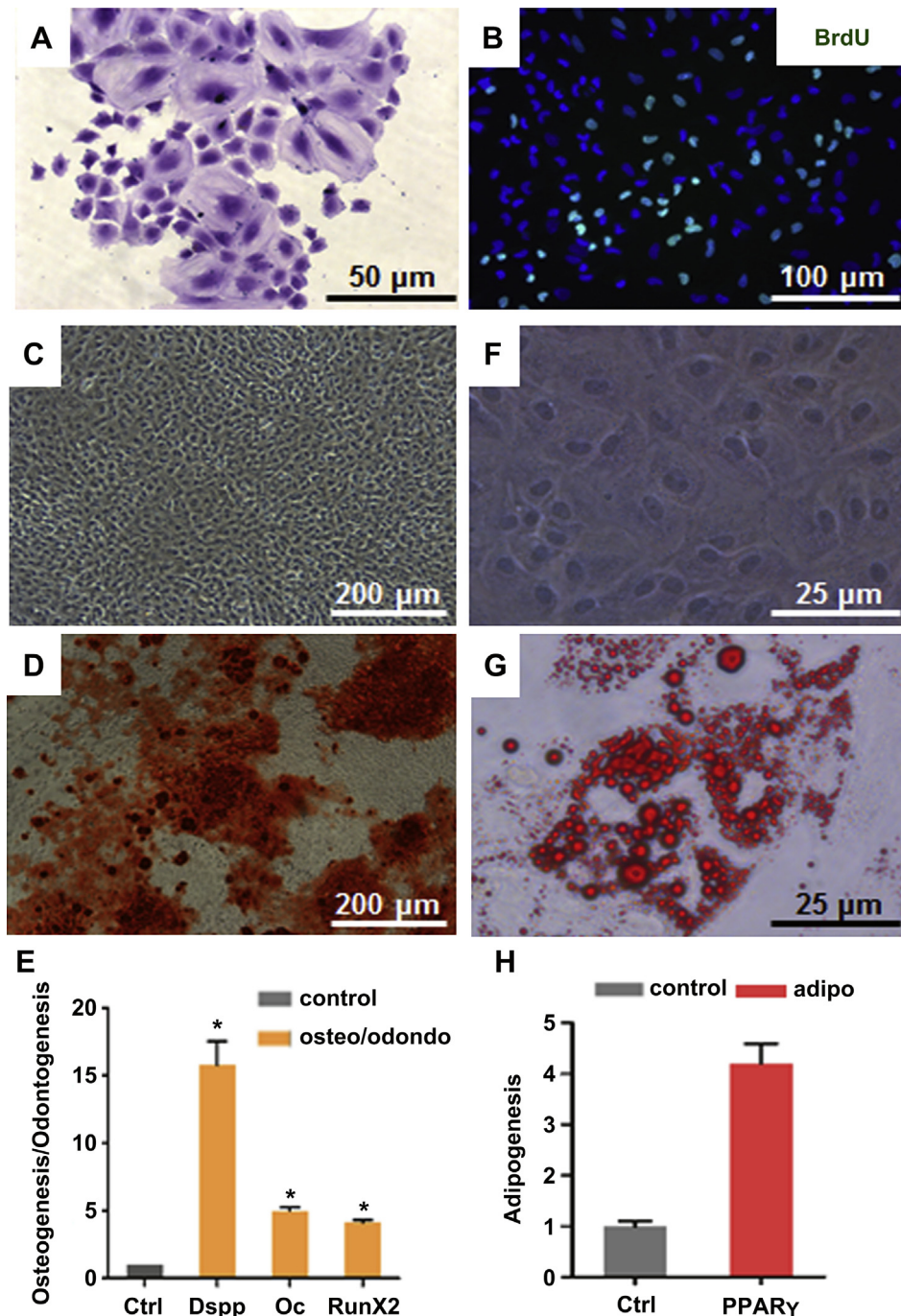


Fig. 3. Confirmation of mesenchyme stem cell phenotype. A) The isolated dental mesenchyme cells formed single colonies. B) Some of the isolated mesenchyme cells were BrdU positive, accounting for 21% of total cells and continued to proliferate in culture (C). D) Dental mesenchyme cells differentiated into osteoblast/odontoblast-like cells and formed mineral nodules and robustly expressed Dspp, osteocalcin and Runx2 (E). G) Dental mesenchyme cells differentiated into adipocyte-like cells and accumulated abundant lipid droplets in addition to robust expression of peroxisome proliferator-activated receptor γ (PPAR γ) (H).

showed significant increases in response to Wnt3a, BMP4 and BMP7 (Fig. 4F). Together, Wnt3a, BMP4 and BMP7 induced robust mRNA expression of Dspp, Alp and osteocalcin in dental mesenchyme cells, suggesting that their corresponding proteins may stimulate dentinogenesis *in vivo*.

We then reconstituted dental epithelium and mesenchyme cells in a collagen gel, and augmented the cells with microencapsulated BMP4, BMP7 and Wnt3a in PLGA microspheres (Fig. 5A) per our prior methods [18], followed by 2-day *in vitro* incubation. Fig. 5B showed the microinjected dental epithelium and mesenchyme cells in a

collagen gel under phase contrast microscopy. Wnt3a, BMP4 and BMP7-primed cells were then transplanted in the renal capsule of athymic nude mice for 8 wks ($N = 4$ per group) (Fig. 5C). Fig. 5D showed release kinetics of BMP4, BMP7 and Wnt3a in PLGA microspheres, with BMP4, BMP7 and Wnt3a released over 80% by 28 days, representing $\frac{1}{2}$ of the time duration of *in vivo* cell implantation for 56 days. Dental epithelium and mesenchyme cells, when stimulated by control-released BMP4, BMP7 and Wnt3a, formed enamel-like (E) and dentin-like (D) tissues in two integrated layers following harvest from *in vivo* implantation (Fig. 5E). Under higher

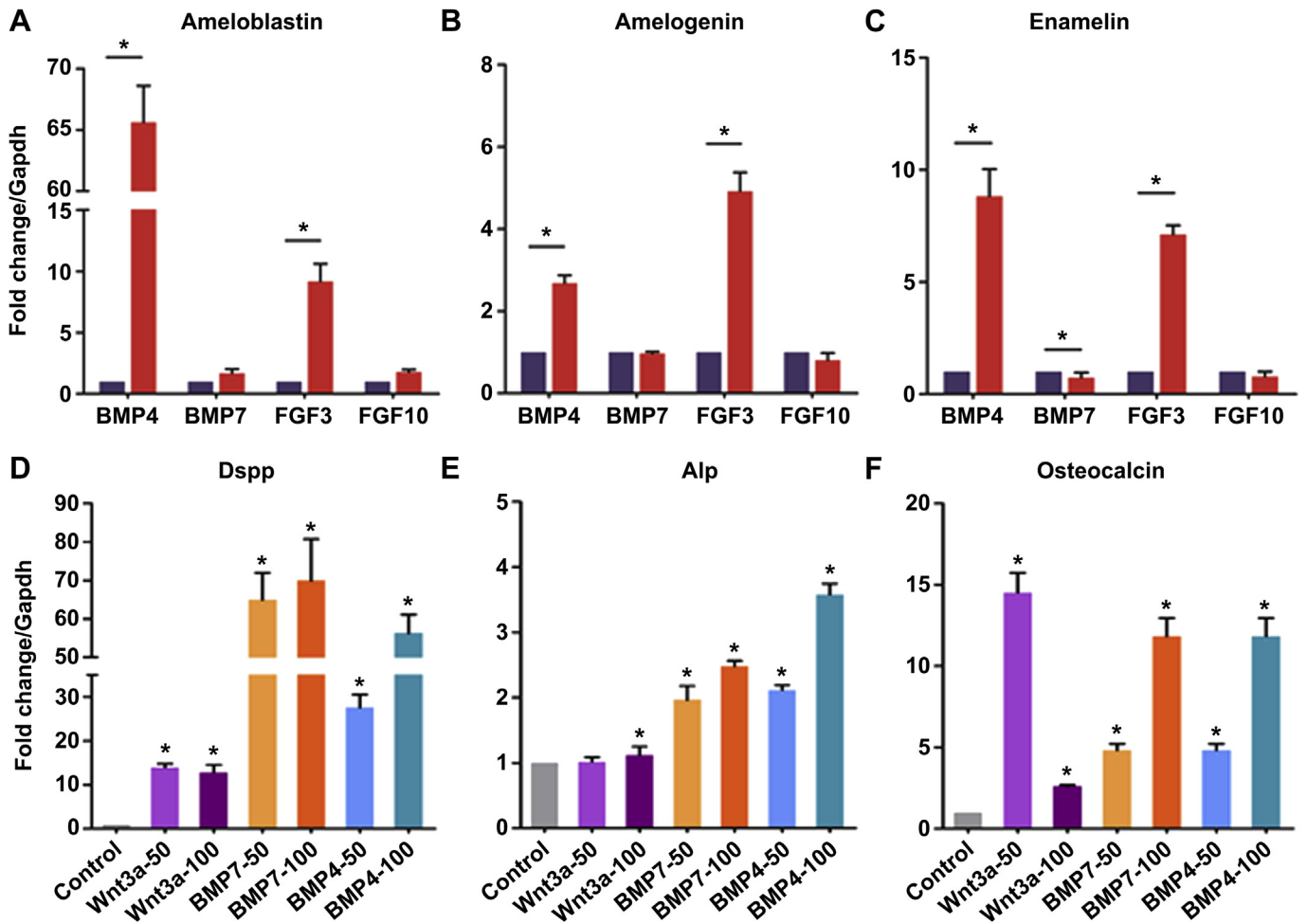


Fig. 4. Augmentation of amelogenesis and odontogenesis transcriptional factors by signaling molecules. BMP4, BMP7, FGF3 and FGF10 up-regulated ameloblastin (A), amelogenin (B) and enamel (C) expression in dental epithelium stem cells. Wnt3a, BMP4 and BMP7 up-regulated Dsp (D), Alp (E) and osteocalcin (F) in dental mesenchyme stem cells.

magnification (of the yellow dashed box in Fig. 5E), enamel-like (E) and dentin-like (D) tissues were observed in two integrated layers and were devoid of any cells, with enamel-like tissue showing more intense HE stain than dentin-like tissue (Fig. 5F). Dentinal-tubule-like structures were present in the regenerated dentin-like tissue and perpendicular to the surface of the enamel-like tissue (Fig. 5F). In contrast, dental epithelium and mesenchyme cells without BMP4, BMP7 and Wnt3a treatment produced irregular mineralized structures (Fig. 5G). When treated by BMP4 alone, dental epithelium and mesenchyme cells produced irregular enamel-like structures but lacked any dentin-like tissue (Fig. 5H). Dental epithelium and mesenchyme cells, when treated by both BMP7 and Wnt3a, yielded areas of mineralization with embedded cells that resemble bone-like or cementum-like structures (Fig. 5I). Immunofluorescence showed that dental epithelium and mesenchyme cells under BMP4, BMP7 and Wnt3a stimulation induced the expression of ameloblastin and amelogenin in the enamel-like tissue (Fig. 6A–C, D–F, respectively) that corresponded to the location of enamel-like tissue in Fig. 5F. BMP4, BMP7 and Wnt3a also induced the expression of dentin sialoprotein (DSP) (Fig. 6G–I), that corresponded to the location of the newly formed dentin-like tissue in Fig. 5F.

4. Discussion

The present findings represent an original discovery of *de novo* amelogenesis and dentinogenesis by postnatal dental epithelium and mesenchyme stem cells based on a classic model of

continuously growing rodent incisor in development. The apical end of the rodent incisor harbors epithelium and mesenchyme stem cells that differentiate into ameloblasts and odontoblasts in development [23]. Our findings show that postnatal 4–5 day dental epithelium and mesenchyme cells in the rodent incisor generate enamel-like and dentin-like tissues *de novo* in two integrated layers when stimulated by BMP4, BMP7 and Wnt3a in the renal capsule. The present data begin to address a critical barrier of a lack of viable postnatal cell sources for tooth regeneration in patients along with parallel attempts of dental pulp/apical stem/progenitor cells [17,24]. The majority of tooth regeneration studies have utilized either E10 dental epithelium or E14.5 dental mesenchyme cells [25,26]. E14.5 cells are equivalent to ~3 month human embryonic tooth germ [27]. Despite the known capacity of embryonic day 10 or day 14.5 mouse tooth germ cells in generating up to an entire tooth organ [10,28], they are not a viable cell source for tooth regeneration in patients. The present findings are pivotal to extend our previous observation that SDF1 and BMP7, when delivered in a 3D-printed, anatomically correct tooth root scaffolds implanted in tooth extraction sockets, promoted mineralized tissue formation with regenerated periodontal ligament and alveolar bone-like structures by the recruitment of host endogenous cells [16,35]. BMP4 and/or Wnt3a, when combined with our previously attempted BMP7, may further augment tooth regeneration. The present findings of Wnt3a and BMP4 in bioengineered amelogenesis and odontogenesis are of particular significance given the paucity of their usage in previous tooth regeneration studies.

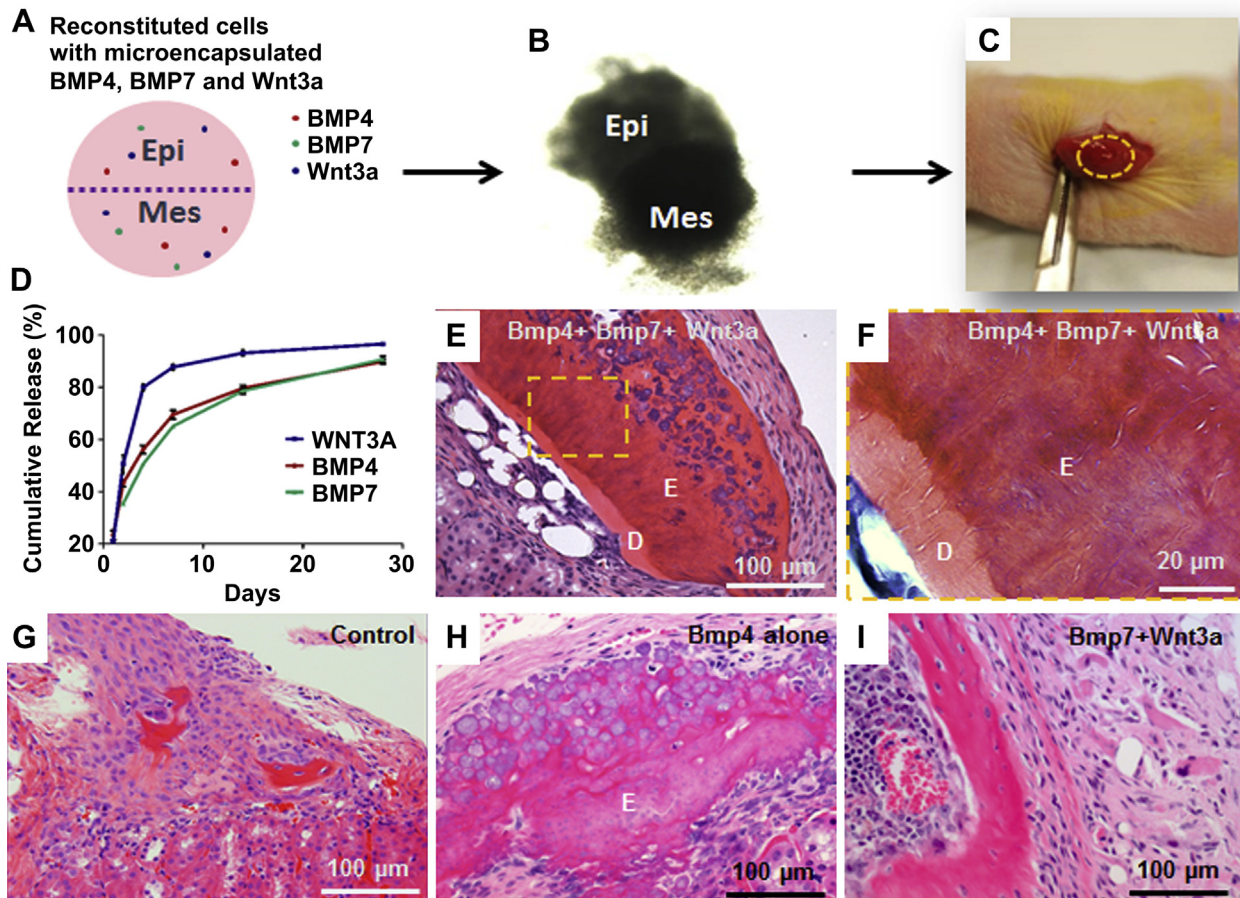


Fig. 5. *In vivo* amelogenesis and odontogenesis. A) Schematics of reconstitution of dental epithelium and mesenchyme cells in two integrated layers of a collagen gel, and augmented the cells with microencapsulated BMP4, BMP7 and Wnt3a in PLGA microspheres. B) Microinjected dental epithelium and mesenchyme stem cells in a collagen gel under phase contrast microcopy. C) Cell/factor loaded gel implanted in the renal capsule of athymic nude mice. D) Release kinetics of BMP4, BMP7 and Wnt3a in PLGA microspheres. E) Enamel-like (E) and dentin-like (D) tissues in two integrated layers following harvest from *in vivo* implantation in renal capsule by dental epithelium and mesenchyme cells, when stimulated by control-released BMP4, BMP7 and Wnt3a. F) Under higher magnification (of yellow dashed box in E), enamel-like (E) and dentin-like (D) tissues integrated in two layers and were devoid of any cells, with enamel-like tissue showing more intense HE stain than dentin-like tissue. G) Dental epithelium and mesenchyme cells in collagen gel, without stimulation by Wnt3a, BMP4 and BMP7, produced irregular, cellular structures of mineralization. H) Irregular enamel-like structures formed by dental epithelium and mesenchyme cells when stimulated by BMP4 alone, but were devoid of any dentin-like tissues. I) Dental epithelium and mesenchyme cells, when stimulated by both BMP7 and Wnt3a, yielded areas of mineralization with embedded cells that resemble bone-like or cementum-like structures.

Previous work has shown that epithelium stem cells in the cervical loop of the rodent incisor undergo rapid proliferation and differentiate into transient amplifying cells, pre-ameloblasts and ameloblasts [3]. However, relatively little is known about the behavior of dental mesenchyme stem cells that surround the cervical loop of the epithelium stem cell niche. We demonstrate that postnatal 4–5 day dental mesenchyme cells in culture, independent of dental epithelium, self-renew to form colonies, readily propagate and differentiate into not only a native lineage of odontoblast-like cells, but also a non-native lineage of adipocytes. These findings of postnatal dental mesenchyme stem/progenitor cells indicate their stemness and potential applications in bioengineered dentinogenesis. Our data further show that postnatal dental epithelium cells in the cervical loop, when separated and cultivated *ex vivo*, retain their epithelium phenotype by sustained CK14 expression, indicating their potential value in bioengineered amelogenesis. Our *in vivo* data, depicting amelogenesis of postnatal dental epithelium cells to yield enamel-like tissue, suggest potential applications in bioengineered enamel formation.

A cascade of signal pathways regulate epithelium and mesenchyme stem/progenitor cells of the rodent incisor including BMP, Wnt, FGF, TGF β , Hedgehog and TNF [29–31]. As a result, the

availability of postnatal dental cells for tooth regeneration not only depends on the cells source but also the right signaling induction to manipulate cells self-renew and differentiation [32]. Here, BMP4, BMP7 and Wnt3a were used to augment epithelium stem cell differentiation towards amelogenesis, and mesenchyme differentiation towards dentin formation. Our findings demonstrate that BMP4 and FGF3 proteins are key promoters of amelogenesis genes including amelogenin, ameloblastin and enamelin, suggesting potential applications of BMP4 and FGF3 along with postnatal epithelium stem/progenitor cells in tooth regeneration. In parallel, we identified that BMP4, BMP7 and Wnt3a proteins are pivotal in up-regulating several odontoblast transcriptional factors and genes including Dspp. These findings are instructive for additional studies to examine the roles played by BMP and Wnt family proteins, along with other key molecules involved in tooth regeneration by postnatal stem/progenitor cells. As an unusual approach among tooth regeneration studies, we microencapsulated BMP4, BMP7 and Wnt3a in PLGA microspheres to potentiate their release in a sustained, controlled fashion. Previous work has shown that delivery of naked proteins and peptides frequently leads to premature diffusion and/or breakdown [19,20]. Potentiated release of BMP4, BMP7 and Wnt3a in the present work likely provided sustained

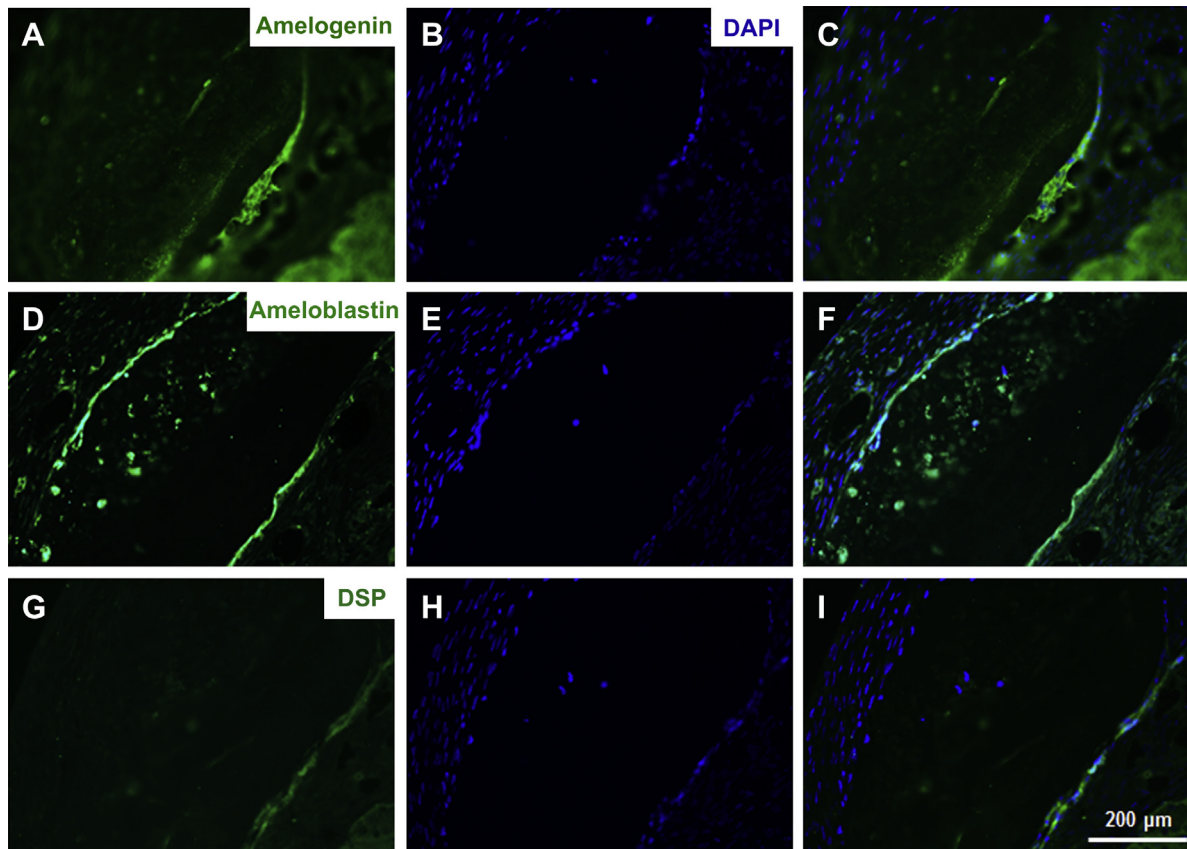


Fig. 6. Immunofluorescence of *in vivo* harvested enamel-like and dentin-like tissues showing amelogenin (A–C), ameloblastin (D–F), and dentin sialoprotein (DSP) (G–I), corresponding to enamel- and dentin-like structures in Fig. 5.

signals for the incorporated postnatal dental epithelium and mesenchyme cells towards amelogenesis and odontogenesis.

The present work was not designed to regenerate an entire tooth organ, since only ectopic implantation of dental epithelium and mesenchyme stem cells were attempted. Epithelium or mesenchyme cells appear to interact within a limited window for the initiation of organogenesis [33]. For example, tooth size and shape are regulated by the enamel knots that determine cusp patterns in the mature tooth [34]. Whether postnatal dental stem/progenitor cells require induction signals for a) initiating amelogenesis and odontogenesis, and b) defining tooth morphogenesis requires additional investigations. Pivotal signals that may equip postnatal stem/progenitor cells with the same capacity as mouse E10 dental epithelium and/or E14.5 dental mesenchyme for tooth organogenesis are evasive and need to be studied.

5. Conclusion

Postnatal dental epithelium stem cells in the cervical loop and the surrounding dental mesenchyme stem cells, when separately microdissected, maintain their phenotypes *ex vivo*. When reconstituted in a collagen gel drop and stimulated by microencapsulated and control-released BMP4, BMP7 and Wnt3a, postnatal dental epithelium and mesenchyme cells orchestrated *de novo* formation of enamel- and dentin-like tissues with dentinal-tubule-like structures in two integrated layers *in vivo*. Given ectopic transplantation in the present study, there is a potential that application of postnatal dental stem/progenitor cells in an orthotopic model, i.e. alveolar bone, may further improve amelogenesis and odontogenesis. Postnatal stem/progenitor cells may serve as an alternative to embryonic tooth germ cells in the regeneration of individual

dental structures such as enamel, cementum, dentin/pulp, or perhaps an entire tooth organ.

Acknowledgments

We thank Ms. Q. Guo and Ms. J. Melendez and for administrative and technical assistance. The effort for composition of this article is supported by NIH grants R01DE023112 and RC2DE020767 to J.J. Mao.

References

- [1] Thesleff I. The genetic basis of tooth development and dental defects. *Am J Med Genet A* 2006;140:2530–5.
- [2] Harada H, Kettunen P, Jung HS, Mustonen T, Wang YA, Thesleff I. Localization of putative stem cells in dental epithelium and their association with notch and FGF signaling. *J Cell Biol* 1999;147:105–20.
- [3] Thesleff I, Tjommers M. Tooth organogenesis and regeneration. Cambridge (MA): StemBook; 2008.
- [4] Hsu YC, Pasolli HA, Fuchs E. Dynamics between stem cells, niche, and progeny in the hair follicle. *Cell* 2011;144:92–105.
- [5] Harada H, Toyono T, Toyoshima K, Yamasaki M, Itoh N, Kato S, et al. FGF10 maintains stem cell compartment in developing mouse incisors. *Development* 2002;129:1533–41.
- [6] Mao JJ, Prockop DJ. Stem cells in the face: tooth regeneration and beyond. *Cell Stem Cell* 2012;11:291–301.
- [7] Kollar EJ, Fisher C. Tooth induction in chick epithelium: expression of quiescent genes for enamel synthesis. *Science* 1980;207:993–5.
- [8] Modino SA, Sharpe PT. Tissue engineering of teeth using adult stem cells. *Arch Oral Biol* 2005;50:255–8.
- [9] Nakao K, Morita R, Saji Y, Ishida K, Tomita Y, Ogawa M, et al. The development of a bioengineered organ germ method. *Nat Methods* 2007;4:227–30.
- [10] Ikeda E, Morita R, Nakao K, Ishida K, Nakamura T, Takano-Yamamoto T, et al. Fully functional bioengineered tooth replacement as an organ replacement therapy. *Proc Natl Acad Sci U S A* 2009;106:13475–80.

- [11] Cai J, Zhang Y, Liu P, Chen S, Wu X, Sun Y, et al. Generation of tooth-like structures from integration-free human urine induced pluripotent stem cells. *Cell Regeneration* 2013;2:6.
- [12] Otsu K, Kishigami R, Oikawa-Sasaki A, Fukumoto S, Yamada A, Fujiwara N, et al. Differentiation of induced pluripotent stem cells into dental mesenchymal cells. *Stem Cells Dev* 2012;21:1156–64.
- [13] Angelova Volponi A, Kawasaki M, Sharpe PT. Adult human gingival epithelial cells as a source for whole-tooth bioengineering. *J Dent Res* 2013;92:329–34.
- [14] Young CS, Terada S, Vacanti JP, Honda M, Bartlett JD, Yelick PC. Tissue engineering of complex tooth structures on biodegradable polymer scaffolds. *J Dent Res* 2002;81:695–700.
- [15] Sumita Y, Honda MJ, Ohara T, Tsuchiya S, Sagara H, Kagami H, et al. Performance of collagen sponge as a 3-D scaffold for tooth-tissue engineering. *Biomaterials* 2006;27:3238–48.
- [16] Kim K, Lee CH, Kim BK, Mao JJ. Anatomically shaped tooth and periodontal regeneration by cell homing. *J Dent Res* 2010;89:842–7.
- [17] Zhang W, Ahluwalia IP, Yelick PC. Three dimensional dental epithelial-mesenchymal constructs of predetermined size and shape for tooth regeneration. *Biomaterials* 2010;31:7995–8003.
- [18] Morotomi T, Kawano S, Toyono T, Kitamura C, Terashita M, Uchida T, et al. In vitro differentiation of dental epithelial progenitor cells through epithelial-mesenchymal interactions. *Arch Oral Biol* 2005;50:695–705.
- [19] Moioli EK, Hong L, Guardado J, Clark PA, Mao JJ. Sustained release of TGFbeta3 from PLGA microspheres and its effect on early osteogenic differentiation of human mesenchymal stem cells. *Tissue Eng* 2006;12:537–46.
- [20] Lee CH, Shah B, Moioli EK, Mao JJ. CTGF directs fibroblast differentiation from human mesenchymal stem/stromal cells and defines connective tissue healing in a rodent injury model. *J Clin Invest* 2010;120:3340–9.
- [21] Wang XP, Suomalainen M, Jorgez CJ, Matzuk MM, Werner S, Thesleff I. Follistatin regulates enamel patterning in mouse incisors by asymmetrically inhibiting BMP signaling and ameloblast differentiation. *Dev Cell* 2004;7:719–30.
- [22] Yokohama-Tamaki T, Ohshima H, Fujiwara N, Takada Y, Ichimori Y, Wakisaka S, et al. Cessation of Fgf10 signaling, resulting in a defective dental epithelial stem cell compartment, leads to the transition from crown to root formation. *Development* 2006;133:1359–66.
- [23] Tummers M, Thesleff I. Root or crown: a developmental choice orchestrated by the differential regulation of the epithelial stem cell niche in the tooth of two rodent species. *Development* 2003;130:1049–57.
- [24] Wei F, Song T, Ding G, Xu J, Liu Y, Liu D, et al. Functional tooth restoration by allogeneic mesenchymal stem cell-based bio-root regeneration in swine. *Stem Cells Dev* 2013;22:1752–62.
- [25] Lumsden AG. Spatial organization of the epithelium and the role of neural crest cells in the initiation of the mammalian tooth germ. *Development* 1988;103(Suppl.):155–69.
- [26] Ohazama A, Modino SA, Miletich I, Sharpe PT. Stem-cell-based tissue engineering of murine teeth. *J Dent Res* 2004;83:518–22.
- [27] Kaufman MH. The atlas of mouse development. London: Academic Press; 1992.
- [28] Thomas HF, Kollar EJ. Differentiation of odontoblasts in grafted recombinants of murine epithelial root sheath and dental mesenchyme. *Arch Oral Biol* 1989;34:27–35.
- [29] Wang XP, Suomalainen M, Felszeghy S, Zelarayan LC, Alonso MT, Plikus MV, et al. An integrated gene regulatory network controls stem cell proliferation in teeth. *PLoS Biol* 2007;5:e159.
- [30] Kassai Y, Munne P, Hotta Y, Penttila E, Kavanagh K, Ohbayashi N, et al. Regulation of mammalian tooth cusp patterning by ectodin. *Science* 2005;309:2067–70.
- [31] Klein OD, Lyons DB, Balooch G, Marshall GW, Basson MA, Peterka M, et al. An FGF signaling loop sustains the generation of differentiated progeny from stem cells in mouse incisors. *Development* 2008;135:377–85.
- [32] Chen X, Zhang T, Shi J, Xu P, Gu Z, Sandham A, et al. Notch1 signaling regulates the proliferation and self-renewal of human dental follicle cells by modulating the G1/S phase transition and telomerase activity. *PLoS One* 2013;8:e69967.
- [33] Cobourne MT, Mitsiadis T. Neural crest cells and patterning of the mammalian dentition. *J Exp Zool B Mol Dev Evol* 2006;306:251–60.
- [34] Jernvall J, Thesleff I. Reiterative signaling and patterning during mammalian tooth morphogenesis. *Mech Dev* 2000;92:19–29.
- [35] Yildirim S, Fu SY, Kim K, Zhou H, Lee CH, Li A, et al. Tooth regeneration: a revolution in stomatology and evolution in regenerative medicine. *Int J Oral Sci* 2011;3:107–16.